JOC Article
pubs.acs.org/joc

Organic Dyes Containing Coplanar Diphenyl-Substituted Dithienosilole Core for Efficient Dye-Sensitized Solar Cells

Li-Yen Lin,[†] Chih-Hung Tsai,[‡] Ken-Tsung Wong,*[,†] Tsung-Wei Huang,[‡] Lun Hsieh,[‡] Su-Hao Liu,[‡] Hao-Wu Lin,[‡] Chung-Chih Wu,*[,‡] Shu-Hua Chou,[†] Shinn-Horng Chen,[§] and An-I Tsai[§]

[†]*Department of Chemistry, National Taiwan University, Taipei 10617, Taiwan,* [‡]*Department of Electrical Engineering, Graduate Institute of Photonics and Optoelectronics, and Graduate Institute of Electronics Engineering, National Taiwan University, Taipei 10617, Taiwan, and* [§]*Energy Material Research Group, Eternal Chemical Co., Ltd., Kaohsiung 821, Taiwan*

kenwong@ntu.edu.tw; chungwu@cc.ee.ntu.edu.tw

Received April 19, 2010

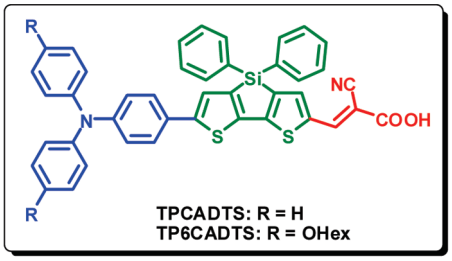

Under AM 1.5G, TP6CADTS-based DSSC gives an overall conversion efficiency of 7.60

Two new organic dyes adopting coplanar diphenyl-substituted dithienosilole as the central linkage have been synthesized, characterized, and used as the sensitizers for dye-sensitized solar cells (DSSCs). The best DSSC exhibited a high power conversion efficiency up to 7.6% (**TP6CADTS**) under AM 1.5G irradiation, reaching ~96% of the ruthenium dye **N719**-based reference cell under the same conditions.

Introduction

Increasing energy demands and concerns about global warming have encouraged scientists to develop cheap and easily accessible renewable energy sources in recent years. In comparison with the traditional silicon-based solar cells,[1] dye-sensitized solar cells (DSSCs) are one of the most promising next-generation photovoltaic cells due to their versatile, energy-saving, and environmentally friendly nature. Therefore, DSSCs have attracted much attention since the breakthrough made by Grätzel et al. in 1991.[2] Several ruthenium-based sensitizers, such as **N3**,[3] **N719**,[4] and black dye,[5] have achieved remarkable power conversion efficiency of 10−11% under standard global air mass 1.5 (AM 1.5G) illumination. However, the rarity and high cost of the ruthenium metal may limit their development for large-scale applications. Consequently, many researchers have focused on developing metal-free organic sensitizers,[7−18] and some of these endeavors have achieved decent efficiencies in the past

(1) Goetzberger, A.; Hebling, C.; Schock, H.-W. *Mater. Sci., Eng. R* **2003**, *40*, 1.
(2) O'Reagen, B.; Grätzel, M. *Nature* **1991**, *353*, 737.
(3) Grätzel, M. *J. Photochem. Photobiol. A* **2004**, *168*, 235.
(4) Nazeeruddin, M. K.; Kay, A.; Rodicio, L.; Humphry-Baker, R.; Müller, E.; Liska, P.; Vlachopoulos, N.; Grätzel, M. *J. Am. Chem. Soc.* **1993**, *115*, 6382.
(5) Nazeeruddin, M. K.; Péchy, P.; Renouard, T.; Zakeeruddin, S. M.; Humphry-Baker, R.; Comte, P.; Liska, P.; Cevey, L.; Costa, E.; Shklover, V.; Spiccia, L.; Deacon, G. B.; Bignozzi, C. A.; Grätzel, M. *J. Am. Chem. Soc.* **2001**, *123*, 1613.
(6) (a) He, Z.; Wong, W.-Y.; Yu, X.; Kwok, H.-S.; Lin, Z. *Inorg. Chem.* **2006**, *45*, 10922. (b) Wong, W.-Y.; Zhou, G.-J.; Yu, X.-M.; Kwok, H.-S.; Tang, B.-Z. *Adv. Funct. Mater.* **2006**, *16*, 838. (c) Zhou, G.; Wong, W.-Y.; Yao, B.; Xie, Z.; Wang, L. *Angew. Chem., Int. Ed.* **2007**, *46*, 1149.
(7) (a) Mishra, A.; Fischer, M. K. R.; Bäuerle, P. *Angew. Chem., Int. Ed.* **2009**, *48*, 2474. (b) Wiberg, J.; Marinado, T.; Hagberg, D. P.; Sun, L.; Hagfeldt, A.; Albinsson, B. *J. Phys. Chem. C* **2009**, *113*, 3881.
(8) (a) Hara, K.; Kurashige, M.; Ito, S.; Shinpo, A.; Suga, S.; Sayama, K.; Arakawa, H. *Chem. Commun.* **2003**, 252. (b) Kitamura, T.; Ikeda, M.; Shigaki, K.; Inoue, T.; Anderson, N. A.; Ai, X.; Lian, T.; Yanagida, S. *Chem. Mater.* **2004**, *16*, 1806.
(9) (a) Hara, K.; Sayama, K.; Ohga, Y.; Shinpo, A.; Suga, S.; Arakawa, H. *Chem. Commun.* **2001**, 569. (b) Hara, K.; Kurashige, M.; Dan-oh, Y.; Kasada, C.; Shinpo, A.; Suga, S.; Sayama, K.; Arakawa, H. *New J. Chem.* **2003**, *27*, 783. (c) Hara, K.; Sato, T.; Katoh, R.; Furube, A.; Ohga, Y.; Shinpo, A.; Suga, S.; Sayama, K.; Sugihara, H.; Arakawa, H. *J. Phys. Chem. B* **2003**, *107*, 597. (d) Wang, Z. S.; Cui, Y.; Hara, K.; Dan-oh, Y.; Kasada, C.; Shinpo, A. *Adv. Mater.* **2007**, *19*, 1138.

Published on Web 06/17/2010 DOI: 10.1021/jo100762t

few years.[10b,c,13c,14b] Among them, the donor−(π-spacer)−acceptor (D−π−A) system is the basic structure for designing the organic sensitizers due to their effective photoinduced intramolecular charge-transfer characteristics. Generally, arylamine-based moieties, which have also been widely used in materials of organic light-emitting diodes (OLEDs), are employed as the electron donor due to the strong electron-donating nature.[6] On the other hand, carboxylic acid, cyanoacrylic acid, or rhodanine-3-acetic acid were introduced into the (D−π−A) system as the electron acceptor as well as the anchoring group to the TiO_2 surface.[7] Various chromophores such as oligoene,[8] coumarin,[9] indoline,[10] oligothiophene,[11] dithienothiophene,[12] thienothiophene,[13] oligophenylenevinylene,[14] fluorene,[15] spirobifluorene,[16] phenoxazine,[17] and triphenylamine[18] have been incorporated as the conjugated spacer between the electron donor and electron acceptor for tuning the wavelength ranges, absorption capability, and other characteristics required for DSSCs.

Among various organic conjugated materials, dithienosilole (DTS) derivatives and dithienosilole-based polymers are promising functional organic materials that have been widely used in organic optoelectronic devices such as light-emitting diodes,[19] field effect transistors,[20] and polymer solar cells.[21] However, there are few reports of utilizing the DTS moiety as the conjugated spacer for the organic sensitizers of DSSCs. During the preparation of this manuscript, Wang et al. reported a sensitizer named **C219** incorporating dihexyl-substituted DTS and 3,4-ethylenedioxythiophene unit as a binary π-conjugated spacer between a lipophilic alkoxy-substituted triphenylamine electron donor and a hydrophilic cyanoacrylic acid electron acceptor, leading to a high efficiency of 10.0−10.3% under AM 1.5 G irradiation.[22] In the meantime, Ko et al. also reported a new class of organic dyes featuring DTS units equipped with various substituents at the 3-position of DTS as D−A spacers and also yielding good efficiencies from 6.73% to 7.50%.[23]

In this paper, we report our design, synthesis, and characterization of two new organic dyes that contain a simple triphenylamine or dihexyloxy-substituted triphenylamine moiety as the electron donor and cyanoacrylic acid as the electron acceptor. These two building blocks are bridged by diphenyl-substituted DTS, which serves as a coplanar π-conjugated spacer to give two organic D−π−A dyes **TPCADTS** and **TP6CADTS** (Scheme 1). We adopted the simple D−π−A structure with a shorter spacer for facilitating the electronic coupling between the electron donor and electron acceptor, resulting in a red-shifted absorption. Hence, efficient harvesting of sunlight can be reasonably anticipated. In addition, the introduction of the diphenyl-substituted DTS as the central linkage for the organic sensitizer possesses two advantages: (1) The HOMO−LUMO gap of DTS is smaller than that of 2,2′-bithiophene and carbon-bridged bithiophene due to the lower lying LUMO,[19b] which in turn originates from the interaction of silicon σ*-orbital and bithiophene π*-orbital, namely, $\sigma^*-\pi^*$ conjugation.[24] The smaller band gap of DTS is highly beneficial for harvesting of sunlight. (2) The tetrahedral silicon center of diphenyl-substituted DTS does not distort the coplanarity of π-conjugated system.[19b] Instead, the diphenyl substitution on silicon atom may reduce the $\pi-\pi$ stacking interactions of dyes and may be beneficial to high electron injection yield and the power conversion efficiency.[25]

(10) (a) Horiuchi, T.; Miura, H.; Sumioka, K.; Uchida, S. *J. Am. Chem. Soc.* **2004**, *126*, 12218. (b) Ito, S.; Zakeeruddin, S. M.; Humphry-Baker, R.; Liska, P.; Charvet, R.; Comte, P.; Nazeeruddin, M. K.; Péchy, P.; Takata, M.; Miura, H.; Uchida, S.; Grätzel, M. *Adv. Mater.* **2006**, *18*, 1202. (c) Ito, S.; Miura, H.; Uchida, S.; Takata, M.; Sumioka, K.; Liska, P.; Comte, P.; Péchy, P.; Grätzel, M. *Chem. Commun.* **2008**, 5194.

(11) (a) Kim, S.; Lee, J. K.; Kang, S. O.; Ko, J.; Yum, J.-H.; Fantacci, S.; De Angelis, F.; Di Censo, D.; Nazeeruddin, M. K.; Grätzel, M. *J. Am. Chem. Soc.* **2006**, *128*, 16701. (b) Choi, H.; Baik, C.; Kang, S. O.; Ko, J.; Kang, M.-S.; Nazeeruddin, M. K.; Grtäzel, M. *Angew. Chem., Int. Ed.* **2008**, *47*, 327. (c) Koumura, N.; Wang, Z.-S.; Mori, S.; Miyashita, M.; Suzuki, E.; Hara, K. *J. Am. Chem. Soc.* **2006**, *128*, 14256. (d) Wang, Z.-S.; Koumura, N.; Cui, Y.; Takahashi, M.; Sekiguchi, H.; Mori, A.; Kubo, T.; Furube, A.; Hara, K. *Chem. Mater.* **2008**, *20*, 3993. (e) Justin Thomas, K. R.; Hsu, Y.-C.; Lin, J. T.; Lee, K.-M.; Ho, K.-C.; Lai, C.-H.; Cheng, Y.-M.; Chou, P.-T. *Chem. Mater.* **2008**, *20*, 1830. (f) Yum, J. H.; Hagberg, D. P.; Moon, S. J.; Karlson, K. M.; Marinado, T.; Sun, L.; Hagfeldt, A.; Nazeeruddin, M. K.; Grätzel, M. *Angew. Chem., Int. Ed.* **2009**, *48*, 1576. (g) Yang, H. Y.; Yen, Y. S.; Hsu, Y. C.; Chou, H. H.; Lin, J. T. *Org. Lett.* **2010**, *12*, 16. (h) Wang, Z.-S.; Koumura, N.; Cui, Y.; Miyashita, M.; Mori, S.; Hara, K. *Chem. Mater.* **2009**, *21*, 2810.

(12) Qin, H.; Wenger, S.; Xu, M.; Gao, F.; Jing, X.; Wang, P.; Zakeeruddin, S. M.; Grätzel, M. *J. Am. Chem. Soc.* **2008**, *130*, 9202.

(13) (a) Xu, M.; Li, R.; Pootrakulchote, N.; Shi, D.; Guo, J.; Yi, Z.; Zakeeruddin, S. M.; Grätzel, M.; Wang, P. *J. Phys. Chem. C* **2008**, *112*, 19770. (b) Zhang, G.; Bai, Y.; Li, R.; Shi, D.; Wenger, S.; Zakeeruddin, S. M.; Grätzel, M.; Wang, P. *Energy Environ. Sci.* **2009**, *2*, 92. (c) Zhang, G.; Bala, H.; Cheng, Y.; Shi, D.; Lv, X.; Yu, Q.; Wang., P. *Chem. Commun.* **2009**, 2198. (d) Choi, H.; Raabe, I.; Kim, D.; Teocoli, F.; Kim, C.; Song, K.; Yum, J. H.; Ko, J.; Nazeeruddin, M. K.; Grätzel, M. *Chem.—Eur. J.* **2010**, *16*, 1193.

(14) (a) Kim, C.; Choi, H.; Kim, S.; Baik, C.; Song, K.; Kang, M. S.; Kang, S. O.; Ko, J. *J. Org. Chem.* **2008**, *73*, 7072. (b) Im, H.; Kim, S.; Park, C.; Jang, S. H.; Kim, C. J.; Kim, K.; Park, N. G.; Kim, C. *Chem. Commun.* **2010**, *46*, 1335.

(15) Justin Thomas, K. R.; Lin, J. T.; Hsu, Y.-C.; Ho, K.-C. *Chem. Commun.* **2005**, 4098.

(16) (a) Cho, N.; Choi, H.; Kim, D.; Song, K.; Kang, M. S.; Kang, S. O.; Ko, J. *Tetrahedron* **2009**, *65*, 6236. (b) Heredia, D.; Natera, J.; Gervaldo, M.; Otero, L.; Fungo, F.; Lin, C.-Y.; Wong, K.-T. *Org. Lett.* **2010**, *12*, 12.

(17) (a) Tian, H.; Yang, X.; Chen, R.; Hagfeldt, A.; Sun, L. *Energy Environ. Sci.* **2009**, *2*, 674. (b) Tian, H.; Yang, X.; Cong, J.; Chen, R.; Liu, J.; Hao, Y.; Hagfeldt, A.; Sun, L. *Chem. Commun.* **2009**, 6288.

(18) (a) Hagberg, D. P.; Edvinsson, T.; Marinado, T.; Boschloo, G.; Hagfeldt, A.; Sun, L. *Chem. Commun.* **2006**, 2245. (b) Hwang, S.; Lee, J. H.; Park, C.; Lee, H.; Kim, C.; Park, C.; Lee, M.-H; Lee, W.; Park, J.; Kim, K.; Park, N.-G.; Kim, C. *Chem. Commun.* **2007**, 4887. (c) Hagberg, D. P.; Marinado, T.; Karlsson, K. M.; Nonomura, K.; Qin, P.; Boschloo, G.; Brinck, T.; Hagfeldt, A.; Sun, L. *J. Org. Chem.* **2007**, *72*, 9550. (d) Liang, M.; Xu, W.; Cai, F.; Chen, P.; Peng, B.; Chen, J.; Li, Z. *J. Phys. Chem. C* **2007**, *111*, 4465. (e) Hagberg, D. P.; Yum, J.-H.; Lee, H.; Angelis, F. D.; Marinado, T.; Karlsson, K. M.; Humphry-Baker, R.; Sun, L.; Hagfeldt, A.; Grätzel, M.; Nazeeruddin, M. K. *J. Am. Chem. Soc.* **2008**, *130*, 6259. (f) Marinado, T.; Nonomura, K.; Nissfolk, J.; Karlsson, M. K.; Hagberg, D. P.; Sun, L.; Mori, S.; Hagfeldt, A. *Langmuir* **2010**, *26*, 2592. (g) Jiang., X.; Marinado, T.; Gabrielsson, E.; Hagberg, D. P.; Sun, L.; Hagfeldt, A. *J. Phys. Chem. C* **2010**, *114*, 2799. (h) Hahlin, M.; Johansson, E. M. J.; Plogmaker, S.; Odelius, M.; Hagberg, D. P.; Sun, L.; Siegbahn, H.; Rensmo, H. *Phys. Chem. Chem. Phys.* **2010**, *12*, 1507.

(19) (a) Ohshita, J.; Nodono, M.; Watanabe, T.; Ueno, Y.; Kunai, A.; Harima, Y.; Yamashita, K.; Ishikawa, M. *J. Organomet. Chem.* **1998**, *553*, 487. (b) Ohshita, J.; Nodono, M.; Kai, H.; Watanabe, T.; Kunai, A.; Komaguchi, K.; Shiotani, M.; Adachi, A.; Okita, K.; Harima, Y.; Yamashita, K.; Ishikawa, M. *Organometallics* **1999**, *18*, 1453. (c) Lee, T.; Jung, I.; Song, K. H.; Lee, H.; Choi, J.; Lee, K.; Lee, B. J.; Park, J. Y.; Lee, C.; Kang, S. O.; Ko, J. *Organometallics* **2004**, *23*, 5280.

(20) (a) Kim, D. H.; Oshita, J.; Lee, K. H.; Kunugi, Y.; Kunai, A. *Organometallics* **2006**, *25*, 1511. (b) Usta, H.; Lu, G.; Facchetti, A.; Marks, T. J. *J. Am. Chem. Soc.* **2006**, *128*, 9034. (c) Beaujuge, P. M.; Pisula, W.; Tsao, H. N.; Ellinger, S.; Müllen, K.; Reynolds, J. R. *J. Am. Chem. Soc.* **2009**, *131*, 7514.

(21) (a) Hou, J.; Chen, H.-Y.; Zhang, S.; Li, G.; Yang, Y. *J. Am. Chem. Soc.* **2008**, *130*, 16144. (b) Huo, L.; Chen, H. Y.; Hou, J.; Chen, T. L.; Yang, Y. *Chem. Commun.* **2009**, 5570.

(22) Zeng, W.; Cao, Y.; Bai, Y.; Wang, Y.; Shi, Y.; Zhang, M.; Wang, F.; Pan, C.; Wang, P. *Chem. Mater.* **2010**, *22*, 1915.

(23) Ko, S.; Choi, H.; Kang, M. S.; Hwang, H.; Ji, H.; Kim, J.; Ko, J.; Kang, Y. *J. Mater. Chem.* **2010**, *20*, 2391.

(24) Yamaguchi, S. *Synth. Met.* **1996**, *82*, 149.

(25) (a) He, J.; Benkö, G.; Korodi, F.; Polívka, T.; Lomoth, R.; Åkermark, B.; Sun, L.; Hagfeldt, A.; Sundström, V. *J. Am. Chem. Soc.* **2002**, *124*, 4922. (b) Wang, Z.-S.; Hara, K.; Dan-oh, Y.; Kasada, C.; Shinpo, A.; Suga, S.; Arakawa, H.; Sugihara, H. *J. Phys. Chem. B* **2005**, *109*, 3907. (c) Wang, X.-F.; Kitao, O.; Zhou, H.; Tamiaki, H.; Sasaki, S.-i. *J. Phys. Chem. C* **2009**, *113*, 7954.

SCHEME 1. Synthesis of Dyes TPCADTS and TP6CADTS

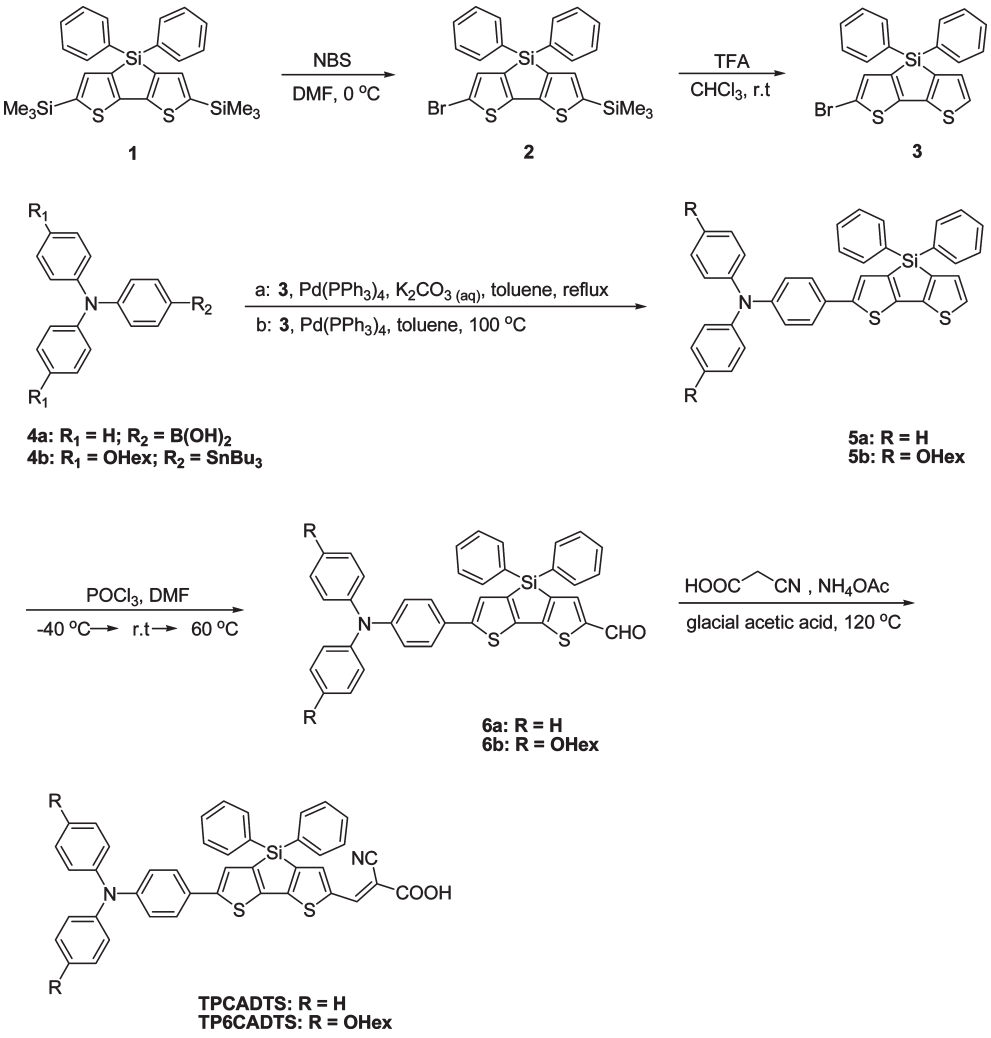

Results and Discussion

The sensitizers **TPCADTS** and **TP6CADTS** were obtained in several steps by the synthetic pathways illustrated in Scheme 1. Different from the two previously reported DTS-containing dyes,[22,23] we adopted 5,5′-bis(trimethylsilyl)-3,3′-diphenylsilylene-2,2′-bithiophene (**1**) as the starting material, which was synthesized according to the published procedures.[19b] Selective monobromination of **1** gave the key intermediate 5-bromo-5′-trimethylsilyl-3,3′-diphenylsilylene-2,2′-bithiophene (**2**) in 66% yield. Compound **2** was then desilylated with TFA to produce 5-bromo-3,3′-diphenylsilylene-2,2′-bithiophene (**3**) with an isolated yield of 98%. The Suzuki cross-coupling reaction of **3** and boronic acids **4a**[26] afforded **5a** in 83% yield, whereas **5b** was synthesized in 61% yield by Stille coupling reaction of **3** with tributyltin-substituted compound **4b**.[27] The free C2-position of DTS core in compound **5** was subsequently converted to their corresponding carbaldehydes **6** by performing the Vilsmeier−Haack reaction, affording **6a** and **6b** in 64% and 78% yield, respectively. Finally, the aldehydes were condensed with cyanoacetic acid to give the target compounds **TPCADTS** and **TP6CADTS** in 85% and 86% yield, respectively, via Knöevenagel reaction in the presence of ammonium acetate.

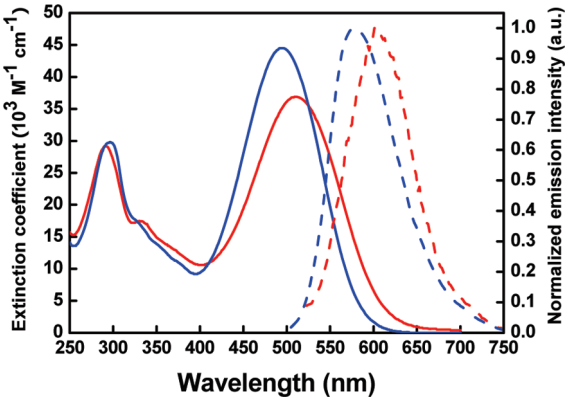

FIGURE 1. Absorption (solid lines) and emission (dashed lines) spectra of **TPCADTS** (blue lines) and **TP6CADTS** (red lines) measured in 2-methyl-2-propanol−acetonitrile (1:1) solution (10^{-5} M).

(26) Li, Z. H.; Wong, M. S. *Org. Lett.* **2006**, *8*, 1499.
(27) Qian, G.; Dai, B.; Luo, M.; Yu, D.; Zhan, J.; Zhang, Z.; Ma, D.; Wang, Z. Y. *Chem. Mater.* **2008**, *20*, 6208.
(28) Hao, Y.; Yang, X.; Cong, J.; Tian, H.; Hagfeldt, A.; Sun, L. *Chem. Commun.* **2009**, 4031.

TABLE 1. Photophysical and Electrochemical Parameters of the Dyes

dye	λ_{abs}[a]/nm	ε[a]/M^{-1} cm^{-1}	λ_{em}[a]/nm	λ_{abs} on TiO_2[b]/nm	E_{0-0}[c]/eV	E_{ox}[d]/V	E_{red}[e]/V	E_{ox}*[f]/V
TPCADTS	495	44500	579	458	1.954	1.065	−0.963	−0.889
TP6CADTS	511	36900	605	470	1.865	0.875	−0.987	−0.99

[a]Absorption and emission spectra were measured in 2-methyl-2-propanol−acetonitrile (1:1) solution (10^{-5} M). [b]Absorption spectra on TiO_2 were obtained through measuring the dye adsorbed on porous TiO_2 nanoparticle film (thickness: 7 μm) in 2-methyl-2-propanol−acetonitrile (1:1) solution. [c]E_{0-0} was estimated from the onset point of the absorption spectra. [d]The oxidation potentials of the dyes were measured in DMF with 0.1 M tetrabutylammonium hexafluorophosphate ($TBAPF_6$) as electrolyte. [e]The reduction potentials of the dyes were measured in THF with 0.1 M tetrabutylammonium perchlorate (TBAP) as electrolyte. For footnotes d and e: working electrode: glassy carbon; reference electrode: Ag/Ag^+; counter electrode: Pt; scan rate: 100 mV/s; calibrated with ferrocene/ferrocenium (Fc/Fc^+) as an internal reference and converted to NHE by addition of 630 mV.[28] [f]$E_{ox}^* = E_{ox} - E_{0-0}$.

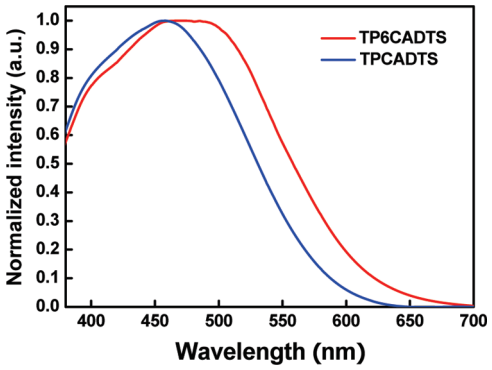

FIGURE 2. Absorption spectra of the dyes anchoring on the 7 μm porous TiO_2 nanoparticle film.

The UV−vis absorption and normalized emission spectra of dyes **TPCADTS** (blue lines) and **TP6CADTS** (red lines) in 2-methyl-2-propanol−acetonitrile (1:1) solution are depicted in Figure 1, and the corresponding data are summarized in Table 1. The absorption spectrum of **TPCADTS** shows an absorption maximum (λ_{max}) centered at 495 nm (ε = 44500 M^{-1} cm^{-1}), which is assigned to the $\pi-\pi^*$ transition. **TP6CADTS** exhibits an absorption λ_{max} at 511 nm (ε = 36900 M^{-1} cm^{-1}) that is red-shifted by 16 nm as compared to that of **TPCADTS** due to the stronger electron-donating nature of hexyloxy substituents. **TPCADTS** and **TP6CADTS** exhibit emission bands centered at 579 and 605 nm, respectively, as excited on their absorption maxima. Upon anchoring on the 7 μm porous TiO_2 nanoparticle film, the absorption maxima of these two dyes show blue-shifted behavior (Figure 2) in comparison with those in 2-methyl-2-propanol−acetonitrile (1:1) solution. The blue shift is attributed to the deprotonation of carboxylic acid upon adsorption onto the TiO_2 surface, and the resulting carboxylate−TiO_2 unit is a weaker electron acceptor compared to the carboxylic acid.[29]

To gain more insight into the electronic structures of **TPCADTS** and **TP6CADTS**, density function theory (DFT) calculations were performed at a B3LYP/6-31G(d) level for the geometry optimization. As shown in Figure 3, the HOMOs of both sensitizers are mainly populated over the triphenylamine and dithienosilole blocks with considerable contribution from the former, whereas LUMOs are delocalized through the dithienosilole and cyanoacrylic acid fragments with sizable contribution from the latter. Examination of the frontier orbitals of both sensitizers suggests that the HOMO−LUMO excitation would shift the electron density distribution from the triphenylamine unit to the cyanoacrylic acid

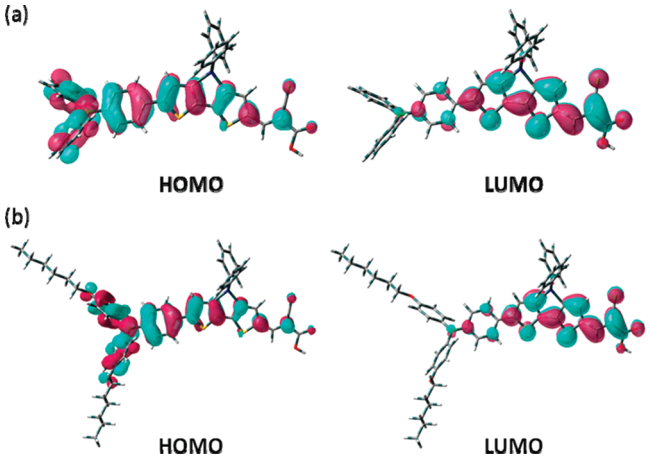

FIGURE 3. Frontier molecular orbitals (HOMO and LUMO) of **TPCADTS** (a) and **TP6CADTS** (b) calculated with DFT on the B3LYP/6-31G(d) level.

moiety, facilitating efficient photoinduced/interfacial electron injection from excited dyes to the TiO_2 electrode.

Quasi-reversible oxidation and reduction waves (E_{ox} and E_{red} in Table 1) were observed for the dyes **TPCADTS** and **TP6CADTS** in the cyclic voltammetry (CV) measurements (Figure 4). The oxidation can be attributed to the triphenylamine moieties, while the reduction can be assigned to the cyanoacrylic acid. Both oxidation and reduction potentials of **TP6CADTS** are more negative than those of **TPCADTS**, yet the difference in reduction potentials of the two dyes is smaller than that in oxidation potentials. It suggests that the introduction of a hexyloxy substituent on the triphenylamine moiety has a significant influence on the ground-state oxidation potential but a more limited effect on the ground-state reduction potential of **TP6CADTS**. The different influence on the ground-state oxidation and reduction potential by incorporating the stronger donor leads to a narrow energy gap of **TP6CADTS**. The zero−zero excitation energy (E_{0-0}) estimated from the absorption onset and the ground-state oxidation potential (E_{ox}) were used to calculate the excited-state oxidation potential (E_{ox}*). The deduced E_{ox}* values of these two dyes are more negative than the conduction band edge of the TiO_2 (−0.5 V vs NHE),[30] indicating that the electron injection process shall be energetically favorable. On the other hand, the ground-state oxidation potentials (E_{ox} in Table 1) of these two dyes are more positive than the redox potential of the iodide/triiodide couple (0.4 V vs NHE). It suggests that the oxidized dyes shall be able to accept

(29) Wang, Z.-S.; Cui, Y.; Dan-oh, Y.; Kasada, C.; Shinpo, A.; Hara, K. *J. Phys. Chem. C* **2007**, *111*, 7224.

(30) Klein, C.; Nazeeruddin, M. K.; Censo, D. D.; Liska, P.; Grätzel, M. *Inorg. Chem.* **2004**, *43*, 4216.

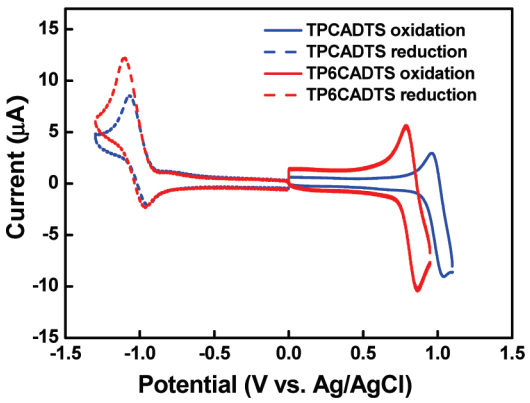

FIGURE 4. Cyclic voltammograms of **TPCADTS** (blue lines) and **TP6CADTS** (red lines); 0.1 M TBAP (reduction) in THF and 0.1 M $TBAPF_6$ (oxidation) in DMF were used as supporting electrolytes. A glassy carbon electrode was used as the working electrode; scan rate: 100 mV/s.

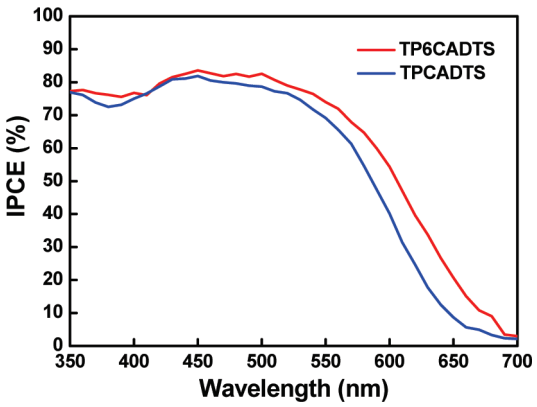

FIGURE 5. IPCE spectra of DSSCs based on **TPCADTS** and **TP6CADTS**.

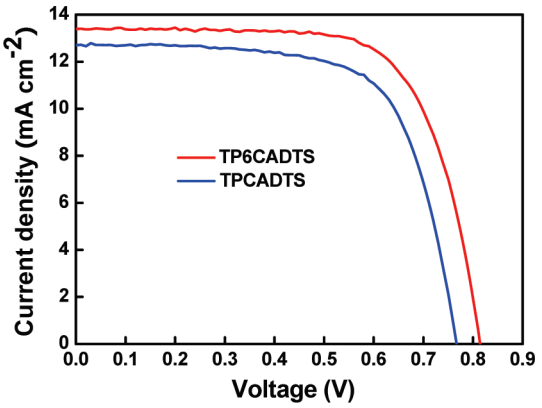

FIGURE 6. Photocurrent density vs voltage for DSSCs based on **TPCADTS** and **TP6CADTS** under AM 1.5 G simulated solar light (100 mW cm^{-2}).

electrons from I^- thermodynamically for effective dye regeneration and to avoid the charge recombination process between oxidized dyes and photoinjected electrons in the TiO_2 film.

The photovoltaic characteristics of **TPCADTS** and **TP6CADTS** as the sensitizers in DSSCs were evaluated with a sandwich DSSC cell comprising 0.6 M 1-butyl-3-methylimidazolium iodide (BMII), 0.05 M LiI, 0.03 M I_2, 0.5 M 4-*tert*-butylpyridine, and 0.1 M guanidinium thiocyanate in a mixture of acetonitrile−valeronitrile (85: 15, v/v) as the redox electrolyte. Details of the device preparation and characterization are described in the Experimental Section. It was reported that the incorporation of 4-*tert*-butylpyridine can decrease the dark current and shift the conduction band edge of the TiO_2 to a more negative potential. As a result, the open-circuit voltage and fill factor can be improved, leading to an improvement on overall conversion efficiencies.[31] The incident monochromatic photon-to-current conversion efficiency (IPCE) spectra of the DSSCs are shown in Figure 5. The IPCE spectrum of **TP6CADTS** is broader than that of **TPCADTS**, as can be expected from the absorption spectrum of **TP6CADTS** anchoring on the 7 μm porous TiO_2 film or its absorption in solutions. The IPCE of **TP6CADTS** exceeds 70% from 350 to 560 nm and reaches a maximum of 84% at 450 nm. Among these two sensitizer dyes, **TP6CADTS** shows higher peak IPCE, although its maximal absorption coefficient may not necessarily be higher than that of **TPCADTS**. The higher peak IPCE of **TP6CADTS** than that of **TPCADTS** may be ascribed to the reduced charge recombination at the TiO_2/dye/electrolyte interface by tailoring with two longer aliphatic hexyloxy chains.[13a]

Figure 6 shows the current−voltage (J−V) curves of the DSSCs under standard global AM 1.5G solar irradiation. The short-circuit photocurrent density (J_{sc}), open-circuit voltage (V_{oc}), and fill factor (ff) of the solar cell based on **TP6CADTS** are 13.39 mA cm^{-2}, 0.81 V, and 0.70, respectively, yielding an overall conversion efficiency (η) of 7.60%. Under the same conditions, the device based on **TPCADTS** shows relatively lower J_{sc} and V_{oc}, leading to an inferior η value of 6.65% (see Table 2). For a fair comparison, the **N719**-sensitized DSSC was also fabricated under the same conditions. The efficiency of the **TP6CADTS**-based cell reaches ~96% of the **N719** cell efficiency (7.93%). The higher J_{sc} value of the **TP6CADTS**-based cell than that of the **TPCADTS**-based cell is consistent with the values for the IPCE spectra, reflecting the better sunlight-harvesting ability of **TP6CADTS**. The two hexyloxy chains of **TP6CADTS** may also contribute to inhibition of dye aggregation and thus to enhancement of J_{sc}.[13a] In addition, with the existence of two aliphatic hexyloxy chains, one also notes that the **TP6CADTS**-based cell gives a 50 mV increase in V_{oc} in comparison with the **TPCADTS**-based cell.

The effects of the two longer hexyloxy chains on photovoltaic characteristics were further elucidated by electrochemical impedance spectroscopy (EIS). The EIS is a useful tool for characterizing important interfacial charge-transfer processes in DSSCs, such as the charge recombination at the TiO_2/dye/electrolyte interface, electron transport in the TiO_2 electrode, electron transfer at the counter electrode, and I_3^- transport in the electrolyte etc.[32−34] In this study, the

(31) (a) Hara, K.; Dan-oh, Y.; Kasada, C.; Ohga, Y.; Shinpo, A.; Suga, S.; Sayama, K.; Arakawa, H. *Langmuir* **2004**, *20*, 4205. (b) Boschloo, G.; Häggman, L.; Hagfeldt, A. *J. Phys. Chem. B* **2006**, *110*, 13144.

(32) Andrade, L.; Zakeeruddin, S. M.; Nazeeruddin, M. K.; Ribeiro, H. A.; Mendes, A.; Grätzel, M. *ChemPhysChem* **2009**, *10*, 1117.

(33) Zhang, J.; Yang, G.; Sun, Q.; Zheng, J.; Wang, P.; Zhu, Y.; Zhao, X. *J. Renewable Sustainable Energy 2* **2010**, 013104.

(34) Fabregat-Santiago, F.; Bisquert, J.; Palomares, E.; Otero, L.; Kuang, D.; Zakeeruddin, S. M.; Gra1tzel, M. *J. Phys. Chem. C* **2007**, *111*, 6550.

TABLE 2. DSSC Performance Parameters of the Dyes[a]

dye	J_{sc}/mA cm^{-2}	V_{oc}/V	ff	η (%)
TPCADTS	12.70	0.76	0.69	6.65
TP6CADTS	13.39	0.81	0.70	7.60
N719	14.65	0.77	0.70	7.93

[a]The concentration of the dyes was maintained at 0.5 mM in 2-methyl-2-propanol−acetonitrile (1:1, v/v) solution, with 0.5 mM deoxycholic acid (DCA) as a co-adsorbent. Performances of DSSCs were measured with a 0.125 cm^2 working area. Irradiating light: AM 1.5 G (100 mW cm^{-2}).

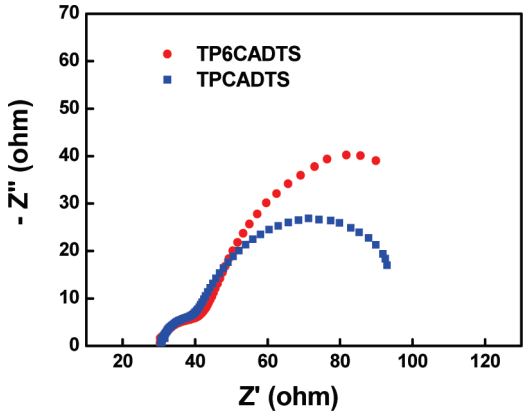

FIGURE 7. EIS Nyquist plots (i.e., minus imaginary part of the impedance $-Z''$ vs the real part of the impedance Z' when sweeping the frequency) for DSSCs based on **TPCADTS** and **TP6CADTS** dyes.

impedance spectroscopy was carried out by subjecting the cell to the constant AM 1.5G 100 mW/cm^2 illumination and to the bias at the open-circuit voltage V_{oc} of the cell (namely, under the conditions of no dc electric current),[34] for better manifesting the process at the TiO_2/electrolyte interface of a cell under operation. Figure 7 shows the EIS Nyquist plots (i.e., minus imaginary part of the impedance $-Z''$ vs the real part of the impedance Z' when sweeping the frequency) for DSSCs based on **TPCADTS** and **TP6CADTS** dyes. For the frequency range investigated (20 Hz to 1 MHz), in both cells, a larger semicircle occurs in the lower frequency range (~20 Hz to 1 kHz) and a smaller semicircle occurs in the higher frequency range. With the bias illumination and voltage applied, the larger semicircle at lower frequencies corresponds to the charge-transfer processes at the TiO_2/dye/electrolyte interface, while the smaller semicircle at higher frequencies corresponds to the charge-transfer processes at the Pt/electrolyte interface. The two cells hardly show a difference in smaller semicircles at higher frequencies, but the difference in larger semicircles at lower frequencies is significant. The larger width of the lower frequency semicircle of the **TP6CADTS** cell indicates a larger charge-transfer resistance at the TiO_2/dye/electrolyte interface.

Figure 8 shows the EIS Bode plots (i.e., the phase of the impedance vs the frequency) of the DSSCs based on **TPCADTS** and **TP6CADTS** dyes. For the frequency range investigated, both EIS Bode plots also exhibit two peak features; the one at higher frequencies corresponds to the charge transfer at the Pt/electrolyte interface and the one at lower frequencies corresponds to the charge transfer at the TiO_2/dye/electrolyte interface. Again, the difference in bode plots of both cells mainly occurs in the lower frequency range. The characteristic frequency of the lower frequency peak in the Bode plot is

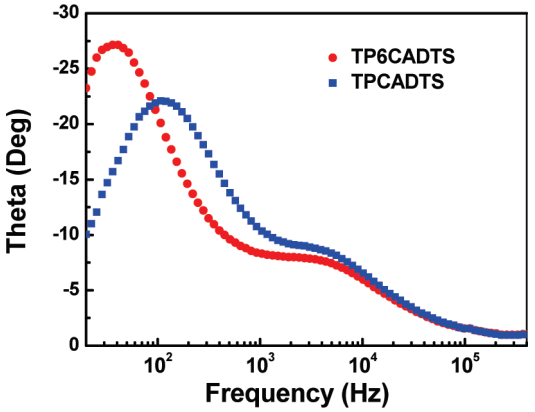

FIGURE 8. EIS Bode plots (i.e., the phase of the impedance vs the frequency) for DSSCs based on **TPCADTS** and **TP6CADTS** dyes.

related to the charge recombination rate, and its reciprocal is associated with the electron lifetime.[35,36] As can be seen in Figure 8, the lower frequency peak of the **TP6CADTS** cell shifts to a lower frequency (compared to the **TPCADTS** cell), indicating that the electron lifetime was effectively prolonged by the two longer hexyloxy chains near the TiO_2/dye/electrolyte interface. EIS results of Figures 7 and 8 clearly suggest that the two longer hexyloxy chains of **TP6CADTS** act as effective blocking units between TiO_2 surface and electrolyte, preventing hydrophilic I_3^- ions approaching the TiO_2 surface and thereby leading to suppressed charge recombination/dark current and lengthened electron lifetimes.[11c,d,37] These factors may in turn lead to the higher V_{oc} (50 mV higher) of the **TP6CADTS** cell than that of the **TPCADTS** cell.

Conclusions

In summary, we had successfully designed and synthesized two new organic sensitizers (**TPCADTS** and **TP6CADTS**) containing coplanar diphenyl-substituted dithienosilole as the central linkage for high-performance dye-sensitized solar cells. By incorporating the diphenyl-substituted DTS core, these two dyes exhibited the enhanced light-capturing abilities and suppressed dye aggregation. These two dyes had been employed as the organic sensitizers in DSSCs. A solar-cell device based on the sensitizer **TP6CADTS** yielded a higher overall conversion efficiency up to 7.6%, reaching ~96% of the ruthenium dye **N719**-based reference cell under the same conditions. The introduction of aliphatic hexyloxy chains on the donor (e.g., **TP6CADTS**) appears to be beneficial to suppression of electronic coupling and charge recombination, etc. at the TiO_2/dye/electrolyte interface, which could contribute to higher V_{oc} and IPCE in DSSCs. The results disclosed in this paper are believed to be useful for further development of other low-cost metal-free organic dyes by different molecular and energy-level engineering processes.

Experimental Section

Synthesis of the Dyes. General Methods. All chemicals and reagents were used as received from commercial sources without

(35) Adachi, M.; Sakamoto, M.; Jiu, J.; Ogata, Y.; Isoda, S. *J. Phys. Chem. B* **2006**, *110*, 13872.
(36) Wang, Q.; Moser, J.; Grätzel, M. *J. Phys. Chem. B* **2005**, *109*, 14945.
(37) Kim, S.; Kim, D.; Choi, H.; Kang, M. S.; Song, K.; Kang, S. O.; Ko, J. *Chem. Commun.* **2008**, 4951.

purification. Solvents for chemical synthesis were purified by distillation. All chemical reactions were carried out under an argon or nitrogen atmosphere.

5-Bromo-5′-trimethylsilyl-3,3′-diphenylsilylene-2,2′-bithiophene (2). To a stirring solution of **1** (13.55 g, 27.60 mmol) in *N*,*N*-dimethylformamide (275 mL) was dropwise added *N*-bromosuccinimide (5.86 g, 33.12 mmol) in *N*,*N*-dimethylformamide (275 mL) at 0 °C under exclusion of light, and the reaction mixture was then warmed to room temperature. After being stirred for 12 h, the reaction mixture was poured into water and extracted with diethyl ether, and the combined extracts were washed with brine, dried over anhydrous magnesium sulfate, and filtered. The solvent was removed by rotary evaporation. The crude product was dissolved in hexane, and the undissolved solid was filtered. The filtrate was evaporated to dryness, and the resulting solid was washed with ethanol to afford **2** as a white solid (9.04 g, 66% yield): mp 140−142 °C; IR (KBr) ν 3065, 2950, 1587, 1427, 1245, 995 cm^{-1}; ^1H NMR ($CDCl_3$, 400 MHz) δ 7.63 (dt, J = 6.4, 1.6 Hz, 4H), 7.45−7.36 (m, 6H), 7.31 (s, 1H), 7.18 (s, 1H), 0.36 (s, 9H); ^{13}C NMR ($CDCl_3$, 100 MHz) δ 154.8, 150.6, 142.5, 140.3, 136.1, 135.2, 132.1, 131.1, 130.3, 128.1, 111.9, 0.3; HRMS (*m*/*z*, FAB^+) calcd for $C_{23}H_{21}BrS_2Si_2$ 495.9807, found 495.9803.

5-Bromo-3,3′-diphenylsilylene-2,2′-bithiophene (3). To a stirring solution of **2** (3.30 g, 6.63 mmol) in chloroform (165 mL) was dropwise added trifluoroacetic acid (0.98 mL, 13.26 mmol) at room temperature under exclusion of light. After being stirred for 12 h, the reaction mixture was poured into water and extracted with chloroform, and the combined extracts were washed with brine, dried over anhydrous magnesium sulfate, and filtered. The solvent was removed by rotary evaporation to afford **3** as a light yellow solid (2.75 g, 98% yield): mp 173−175 °C; IR (KBr) ν 3090, 3018, 1586, 1427, 1250, 943 cm^{-1}; ^1H NMR ($CDCl_3$, 400 MHz) δ 7.64 (d, J = 6.8 Hz, 4H), 7.47−7.37 (m, 6H), 7.30 (d, J = 4.8 Hz, 1H), 7.24 (d, J = 4.8 Hz, 1H), 7.20 (s, 1H); ^{13}C NMR ($CDCl_3$, 100 MHz) δ 150.5, 149.6, 139.9, 138.7, 135.2, 132.0, 130.9, 130.4, 129.5, 128.1, 126.2, 111.8; HRMS (*m*/*z*, FAB^+) calcd for $C_{20}H_{13}BrS_2Si$ 423.9411, found 423.9416.

5-[*N*,*N*-Bis(phenylamino)phenyl]-3,3′-diphenylsilylene-2,2′-bithiophene (5a). A mixture of **3** (2.33 g, 5.48 mmol), **4a** (1.90 g, 6.58 mmol), tetrakis(triphenylphosphine)palladium(0) (316 mg, 0.27 mmol), and potassium carbonate (2 M aqueous solution, 13.7 mL, 27.40 mmol) in toluene (270 mL) was stirred and heated to reflux under argon for 2.5 h. The reaction mixture was poured into water and extracted with dichloromethane, and the combined extracts were washed with brine, dried over anhydrous magnesium sulfate, and filtered. The solvent was removed by rotary evaporation, and the crude product was purified by column chromatography on silica gel with dichloromethane/hexane (v/v, 1:5) as eluent to afford **5a** as a yellow solid (2.68 g, 83% yield): mp 230−232 °C; IR (KBr) ν 3059, 3023, 1590, 1494, 1273, 826 cm^{-1}; ^1H NMR ($CDCl_3$, 400 MHz) δ 7.67 (dt, J = 6.4, 1.6 Hz, 4H), 7.48−7.22 (m, 15 H), 7.12 (dd, J = 8.4, 1.2 Hz, 4H), 7.07−7.02 (m, 4H); ^{13}C NMR ($CDCl_3$, 100 MHz) δ 150.5, 148.4, 147.3, 146.9, 145.7, 141.1, 139.0, 135.3, 131.6, 130.2, 129.5, 129.2, 128.4, 128.1, 126.3, 125.8, 124.6, 124.3, 123.6, 122.9; HRMS (*m*/*z*, FAB^+) calcd for $C_{38}H_{27}NS_2Si$ 589.1354, found 589.1349.

5-[*N*,*N*-Bis(4-hexyloxyphenylamino)phenyl]-3,3′-diphenylsilylene-2,2′-bithiophene (5b). A mixture of **3** (2.94 g, 6.91 mmol), **4b** (7.61 g, 10.37 mmol), tetrakis(triphenylphosphine)palladium(0) (404 mg, 0.35 mmol) in toluene (35 mL) was stirred and heated at 100 °C under argon for 24 h. After the mixture was cooled to room temperature, the solvent was removed by rotary evaporation, and the crude product was purified by column chromatography on silica gel with dichloromethane/hexane (v/v, 1:3) as eluent to afford **5b** as a yellow solid (3.32 g, 61% yield): mp 55−57 °C; IR (KBr) ν 3063, 2955, 2853, 1601, 1505, 1475, 1011, 824 cm^{-1}; ^1H NMR (DMSO-d_6, 400 MHz) δ 7.71 (s, 1H), 7.66 (d, J = 6.8 Hz, 4H), 7.56 (d, J = 4.4 Hz, 1H), 7.50−7.37 (m, 9H), 6.99 (d, J = 8.8 Hz, 4H), 6.87 (d, J = 8.8 Hz, 4H), 6.75 (d, J = 8.4 Hz, 2H), 3.89 (t, J = 6.2 Hz, 4H), 1.67 (m, 4H), 1.38 (m, 4H), 1.29 (m, 8H), 0.86 (t, J = 6.2 Hz, 6H); ^{13}C NMR (CD_2Cl_2, 100 MHz) δ 156.1, 151.0, 148.7, 148.2, 146.8, 141.6, 140.6, 139.3, 135.7, 132.2, 130.7, 130.0, 128.6, 127.2, 126.6, 126.4, 126.3, 124.4, 120.4, 115.7, 68.8, 32.2, 29.9, 26.4, 23.3, 14.5; HRMS (*m*/*z*, FAB^+) calcd for $C_{50}H_{51}NO_2S_2Si$ 789.3130, found 789.3133.

5-[*N*,*N*-Bis(phenylamino)phenyl]-5′-formyl-3,3′-diphenylsilylene-2,2′-bithiophene (6a). To a stirring solution of **5a** (826 mg, 1.4 mmol) in dry *N*,*N*-dimethylformamide (30 mL) was dropwise added phosphorus oxychloride (0.22 mL, 2.38 mmol) at −40 °C under argon. The reaction mixture was then heated to 60 °C and stirred for 4 h. After being cooled to room temperature, the reaction mixture was quenched with 10% sodium acetate aqueous solution (210 mL) and extracted with ethyl acetate, and the combined extracts were washed with brine, dried over anhydrous magnesium sulfate, and filtered. The solvent was removed by rotary evaporation, and the crude product was purified by column chromatography on silica gel with ethyl acetate/hexane (v/v, 1:10) as eluent to afford **6a** as a red solid (553 mg, 64% yield): mp 235−237 °C; IR (KBr) ν 3031, 2809, 1657, 1589, 1487, 1115, 825 cm^{-1}; ^1H NMR ($CDCl_3$, 400 MHz) δ 9.87 (s, 1H), 7.86 (s, 1H), 7.65 (dd, J = 8.0, 1.2 Hz, 4H), 7.49−7.45 (m, 4H), 7.41−7.37 (m, 5H), 7.30−7.26 (m, 4H), 7.12 (dd, J = 8.4, 0.8 Hz, 4H), 7.08−7.04 (m, 4H); ^{13}C NMR ($CDCl_3$, 100 MHz) δ 182.2, 159.7, 149.9, 147.8, 147.1, 146.7, 145.8, 144.7, 139.9, 139.4, 135.2, 130.7, 130.2, 129.2, 128.3, 127.3, 126.7, 124.9, 124.6, 123.3, 123.1; HRMS (*m*/*z*, FAB^+) calcd for $C_{39}H_{27}NOS_2Si$ 617.1303, found 617.1304.

5-[*N*,*N*-Bis(4-hexyloxyphenylamino)phenyl]-5′-formyl-3,3′-diphenylsilylene-2,2′-bithiophene (6b). To a stirring solution of **5b** (2 g, 2.53 mmol) in dry *N*,*N*-dimethylformamide (54 mL) was dropwise added phosphorus oxychloride (0.4 mL, 4.3 mmol) at −40 °C under argon. The reaction mixture was then heated to 60 °C and stirred for 3 h. After being cooled to room temperature, the reaction mixture was quenched with 10% sodium acetate aqueous solution (380 mL) and extracted with ethyl acetate, and the combined extracts were washed with brine, dried over anhydrous magnesium sulfate, and filtered. The solvent was removed by rotary evaporation, and the crude product was purified by column chromatography on silica gel with ethyl acetate/hexane (v/v, 1:10) as eluent to afford **6b** as a red solid (1.62 g, 78% yield): mp 65−67 °C; IR (KBr) ν 3061, 2953, 2856, 2706, 1664, 1599, 1506, 1237, 1139, 825 cm^{-1}; ^1H NMR (DMSO-d_6, 400 MHz) δ 9.87 (s, 1H), 8.40 (s, 1H), 7.86 (s, 1H), 7.70 (d, J = 7.2 Hz, 4H), 7.55−7.41 (m, 8H), 7.03 (d, J = 8.8 Hz, 4H), 6.90 (d, J = 8.8 Hz, 4H), 6.74 (d, J = 8.4 Hz, 2H), 3.92 (t, J = 6.8 Hz, 4H), 1.69 (m, 4H), 1.39 (m, 4H), 1.30 (m, 8H), 0.87 (t, J = 6.8 Hz, 6H); ^{13}C NMR (CD_2Cl_2, 100 MHz) δ 182.6, 159.9, 156.4, 150.9, 149.4, 146.5, 146.4, 145.2, 140.3, 140.2, 139.8, 135.7, 131.1, 130.9, 128.7, 127.5, 126.9, 125.5, 124.7, 119.9, 115.7, 68.8, 32.2, 29.9, 26.3, 23.3, 14.5; HRMS (*m*/*z*, FAB^+) calcd for $C_{51}H_{51}NO_3S_2Si$ 817.3080, found 817.3077.

3-[5-[*N*,*N*-Bis(phenylamino)phenyl]-3,3′-diphenylsilylene-2,2′-bithiophene-5′-yl]-2-cyanoacrylic Acid (TPCADTS). A mixture of **6a** (370 mg, 0.6 mmol), cyanoacetic acid (153 mg, 1.8 mmol), and ammonium acetate (39 mg) in glacial acetic acid (13 mL) was stirred and heated at 120 °C for 12 h. After the mixture was cooled to room temperature, the resulting precipitate was collected by filtration and thoroughly washed with water, methanol, and diethyl ether to afford **TPCADTS** as a black solid (350 mg, 85% yield): mp 294−296 °C; IR (KBr) ν 3056, 2217, 1718, 1682, 1592, 1429, 824 cm^{-1}; ^1H NMR (DMSO-d_6, 400 MHz) δ 8.46 (s, 1H), 8.32 (s, 1H), 7.96 (s, 1H), 7.69−7.64 (m, 6H), 7.52−7.48 (m, 2H), 7.46−7.42 (m, 4H), 7.35−7.31 (m, 4H), 7.11−7.05 (m, 6H), 6.97 (d, J = 8.8 Hz, 2H); ^{13}C NMR (DMSO-d_6, 100 MHz) δ 163.8, 158.8, 149.8, 147.5, 146.6, 146.4, 145.5, 143.4, 139.8, 137.3, 135.0, 130.9, 129.9, 129.7, 128.5, 126.9, 126.6, 126.3, 124.6, 123.7, 122.5, 116.9; HRMS (*m*/*z*, FAB^+) calcd for $C_{42}H_{28}N_2O_2S_2Si$ 684.1361, found 684.1357.

3-[5-[*N*,*N*-Bis(4-hexyloxyphenylamino)phenyl]-3,3′-diphenylsilylene-2,2′-bithiophene-5′-yl]-2-cyanoacrylic Acid (TP6CADTS). A mixture of **6b** (327 mg, 0.4 mmol), cyanoacetic acid (102 mg, 1.2 mmol), and ammonium acetate (26 mg) in glacial acetic acid (9 mL) was stirred and heated at 120 °C for 12 h. After being cooled to room temperature, the resulting precipitate was collected by filtration and thoroughly washed with water, methanol, and hexane to afford **TP6CADTS** as a black solid (305 mg, 86% yield): mp 244−246 °C; IR (KBr) ν 3062, 2930, 2854, 2215, 1719, 1682, 1565, 1373, 822 cm^{-1}; ^1H NMR (DMSO-d_6, 400 MHz) δ 8.46 (s, 1H), 8.31 (s, 1H), 7.87 (s, 1H), 7.67 (d, J = 7.2 Hz, 4H), 7.56−7.42 (m, 8H), 7.03 (d, J = 8.8 Hz, 4H), 6.90 (d, J = 8.8 Hz, 4H), 6.75 (d, J = 8.4 Hz, 2H), 3.92 (t, J = 6.8 Hz, 4H), 1.69 (m, 4H), 1.40 (m, 4H), 1.30 (m, 8H), 0.88 (t, J = 6.8 Hz, 6H); ^{13}C NMR (DMSO-d_6, 100 MHz) δ 164.5, 156.3, 151.2, 149.4, 147.2, 145.5, 140.3, 139.9, 137.8, 135.7, 131.6, 130.7, 129.2, 127.8, 127.4, 126.2, 124.9, 119.3, 116.2, 68.3, 31.7, 29.4, 25.9, 22.7, 14.6; HRMS (m/z, FAB^+) calcd for $C_{54}H_{52}N_2O_4S_2Si$ 884.3138, found 884.3146.

Theoretical Calculation. Density functional theory (DFT) calculations were conducted by using the B3LYP hybrid functional for the geometry optimizations. The molecular orbital levels of HOMO and LUMO were achieved with the 6-31G(d) basis set implemented in the Gaussian 03 package.

Measurement of Absorption Spectra of Dye-Loaded Nanoporous TiO_2 Films. A 7 μm thick transparent porous TiO_2 nanoparticle layer (adopting 20 nm anatase TiO_2 nanoparticles) was coated on a glass plate by the doctor-blade method. After being sintered at 500 °C for 30 min, the TiO_2 film was immersed into the dye solutions of 0.5 mM dye in acetonitrile and 2-methyl-2-propanol (volume ratio 1:1) at room temperature for 24 h. The UV−vis absorption spectrum of the dye-loaded TiO_2 film was then recorded on a spectrophotometer.

Fabrication of Dye-Sensitized Solar Cells. To prepare the DSSC working electrodes, the FTO glass plates were first cleaned in a detergent solution using an ultrasonic bath for 15 min and then rinsed with water and ethanol. A layer of 20 nm anatase TiO_2 nanoparticles for the transparent nanocrystalline layer was first coated on the FTO glass plates by the doctor-blade method. After the film was dried at 120 °C, another layer of 400 nm anatase TiO_2 nanoparticles was then deposited as the light-scattering layer of the DSSC. The resulting working electrode was composed of a 7 μm thick transparent TiO_2 nanoparticle layer (particle size: 20 nm) and a 5 μm thick TiO_2 scattering layer (particle size: 400 nm). The nanoporous TiO_2 electrodes were then sequentially heated at 150 °C for 10 min, at 300 °C for 10 min, at 400 °C for 10 min, and finally, at 500 °C for 30 min. After cooling, the nanoporous TiO_2 electrodes were immersed into the dye solutions of 0.5 mM dye and 0.5 mM deoxycholic acid (DCA) in acetonitrile and 2-methyl-2-propanol (volume ratio 1:1) at room temperature for 24 h. Counterelectrodes of the DSSC were prepared by depositing 40 nm thick Pt films on the FTO glass plates by e-beam evaporation. The dye-adsorbed TiO_2 working electrode and a counter electrode were then assembled into a sealed DSSC cell with a sealant spacer between the two electrode plates. A drop of electrolyte solution [0.6 M 1-butyl-3-methylimidazolium iodide (BMII), 0.05 M LiI, 0.03 M I_2, 0.5 M 4-*tert*-butylpyridine, and 0.1 M guanidinium thiocyanate in a mixture of acetonitrile−valeronitrile (85:15, v/v)] was injected into the cell through a drilled hole. Finally, the hole was sealed using the sealant and a cover glass. A mask with an aperture area of 0.125 cm^2 was covered on a testing cell during photocurrent−voltage and incident photon-to-current conversion efficiency measurements.

Photocurrent−Voltage Measurement. The photocurrent−voltage characteristics of the DSSCs were measured under illumination of AM1.5G solar light from a 300-W xenon lamp solar simulator. The incident light intensity was calibrated as 100 mW/cm^2. Photocurrent−voltage curves were obtained by applying an external bias voltage to the cell and measuring the generated photocurrent.

Incident Monochromatic Photon-to-Current Conversion Efficiency Measurement. The incident monochromatic photon-to-current conversion efficiency (IPCE) spectra were measured by using a 75-W xenon lamp as the light source coupled to a monochromator.[38] The IPCE data were taken by illuminating monochromatic light on the solar cells (with a wavelength sampling interval of 10 nm from 350 to 700 nm) and measuring the short-circuit current of the solar cells. The IPCE measurement was performed with a lock-in amplifier, a low-peed chopper, and a bias light source under full computer control.

Electrochemical Impedance Spectroscopy Measurement. The electrochemical impedance spectroscopy (EIS) of the cells was measured by using an impedance analyzer with a frequency range of 20 Hz to 1 MHz. In this study, during the impedance measurement, the cell was under the constant AM 1.5G 100 mW/cm^2 illumination. The impedance of the cell (throughout the frequency range of 20 Hz to 1 MHz) was then measured by applying a bias at the open-circuit voltage V_{oc} of the cell (namely, under the condition of no dc electric current) and by using an ac amplitude of 10 mV.

Acknowledgment. This work was financially supported by the National Science Council of Taiwan.

Supporting Information Available: ^1H and ^{13}C NMR spectra for all new compounds. This material is available free of charge via the Internet at http://pubs.acs.org.

(38) (a) Lin, H.-W.; Ku, S.-Y.; Su, H.-C.; Huang, C.-W.; Lin, Y.-T.; Wong, K.-T.; Wu, C.-C. *Adv. Mater.* **2005**, *17*, 2489. (b) Yang, C.-J.; Cho, T.-Y.; Lin, C.-L.; Wu, C.-C. *Appl. Phys. Lett.* **2007**, *90* (17), 173507. (c) Yang, C.-Y.; Cho, T.-Y.; Chen, Y.-Y.; Yang, C.-J.; Meng, C.-Y.; Yang, C.-H.; Yang, P.-C.; Wu, C.-C.; Lee, S.-C. *Appl. Phys. Lett.* **2007**, *90* (23), 233512. (d) Yang, C.-J.; Cho, T.-Y.; Lin, C.-L.; Wu, C.-C. *J. Soc. Inf. Display* **2008**, *16* (6), 691.